SF2A 2023
M. N'Diaye, A. Siebert, N. Lagarde, O. Venot, K. Baillié, M. Béthermin, E. Lagadec, J. Malzac, J. Richard (eds)

MULTI-WAVELENGTH EMISSION OF FR 0 RADIO GALAXIES AT THE SUBPARSEC SCALE

M. Boughelilba[1]

Abstract. Fanaroff-Riley (FR) 0 radio galaxies are a new class of radio galaxies. These sources are usually weaker but much more numerous than the well-established class of FR I and FR II radio galaxies. In particular, they are observationally very close to the FR I radio galaxies, with the exception of the lack of extended radio emission. We propose a lepto-hadronic jet model, focusing on the core emission region, with parameters close to equipartition, combined with an advection-dominated accretion flow model. This model was successfully used for the FR I galaxy M87 in order to explain its quiet core emission. This combined model is able to reproduce the multiwavelength FR 0 data, both for the gamma-ray undetected sources, as well as the two sources recently associated with a Fermi-LAT detection.

Keywords: Relativistic jets, Particle astrophysics, Active galactic nuclei, High energy astrophysics, Gamma-ray sources

1 Introduction

Based on their radio morphology, radio galaxies are usually classified as either faint edge-darkened Fanaroff-Riley type I (FR I) or bright edge-brightened type II (FR II) galaxies. Recently, a new type of radio galaxy has gained popularity, named FR 0 galaxies (Baldi et al. 2018). From the radio perspective, FR 0s are similar to FR Is, except for the lack of extended emission (i.e. on a kiloparsec scale). Optical and X-ray observation (Torresi et al. 2018), confirm the similarity of the nuclear properties of the two classes. In the high-energy domain, the detection of gamma rays FR 0s (namely LEDA 55267 and LEDA 58287) has recently been reported in Paliya (2021). As of now the population is characterized by a redshift z $\leq$ 0.05, radio sources located at maximum 2" from the optical centre, a minimum FIRST flux of 5 mJy at 1.4 GHz. FR 0s are shown to be in the order of $\sim$ 5 times more numerous than the FR I radio galaxies in the local Universe, making them the dominating jet population there (Baldi & Capetti 2009, 2010). Several hypotheses have been proposed so far, to explain the lack of extended radio emission from FR 0s (Baldi et al. 2019; Garofalo et al. 2010; Garofalo & Singh 2019). We propose that the true nature of this jet population is linked to their broadband spectral energy distribution (SED). Here, we compare the broadband emission of FR 0s to FR Is, and in particular to M87 as one of the most detailed studied archetypal FR I galaxy.

2 Broadband SED

Following Merten et al. (2021) we collected available data from 114 FR 0s. The gamma-ray data of LEDA 55267 and LEDA 58287 are taken from Paliya (2021). We also collected data of 216 FR I sources listed in the FRICAT (Capetti et al. 2017) in the same way. These data are compared to M87's quiet core emission from 2017 (EHT MWL Science Working Group et al. 2021) and its multiwavelength flaring state. We use the average fitted values and uncertainties reported all together in MAGIC Collaboration et al. (2020). Figure 1 shows the resulting broadband SEDs of FR 0s as compared to those of M87 and all the other FR Is, all scaled to the mean distance of FR 0s (i.e $z \sim 0.04$). What stands out in this comparison is the extreme similarity between M87's quiet core emission and the spectral behaviour of FR 0s, at all wavelengths. A model that reproduces the radio-to-gamma-ray quiet core emission of M87 in a one-zone setup was proposed by Boughelilba et al. (2022). This model focuses on the central region of the AGN, with a jet emission region of a few gravitational radii. Given the compactness of the FR 0s and the SED similarities, we explore here the same type of model for the FR 0 source class.

[1] Universität Innsbruck, Institut für Astro- und Teilchenphysik, 6020 Innsbruck, Austria

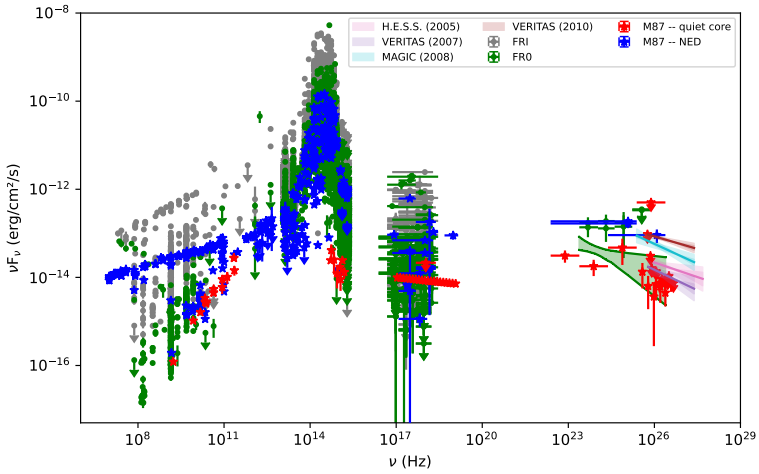

Fig. 1. Broadband SED of FR Is (grey dots), FR 0s (green dots and green butterfly), M87 in its 2017 quiet state (red stars). The blue star symbols are the SED of M87 with all the observations available in the NED. The butterfly plots in the very-high-energy gamma-ray range are the power-law spectra fitted to observations of the flaring state of M87 with H.E.S.S (Aharonian et al. 2006, pink region), VERITAS (Acciari et al. 2008; Aliu et al. 2012, purple and brown regions respectively) and with MAGIC (Albert et al. 2008; MAGIC Collaboration et al. 2020, cyan region). The fluxes from FR Is and M87 have been rescaled from their mean distance to the mean distance of FR 0s.

3 Model

We consider a continuous cylindrical jet of radius $R'_{\rm em}$ containing primary relativistic electrons and protons that are isotropically and homogeneously distributed in the comoving jet frame, and follow a power-law energy spectrum cutting off exponentially, such that the spectral number density $n'_{e,p}(E') \propto E'^{-p_{e,p}} e^{-E'/E'_{{\rm max},e,p}}$ cm^{-3}, for $E' \geq E'_{{\rm min},e,p}$ (where e,p denotes the electrons or the protons, respectively). The primary particles are continuously injected into the emission region, where they experience energy losses caused by various interactions. Specifically, we consider photo-meson production, Bethe-Heitler pair production, inverse-Compton scattering, γ-γ pair production, decay of all unstable particles, synchrotron radiation (from electrons and positrons, protons, and $\pi^\pm$, $\mu^\pm$ and $K^\pm$ before their respective decays), and particle escape.

We model Advection-Dominated Accretion Flows (ADAFs, Rees et al. 1982; Ichimaru 1977; Narayan & Yi 1995; Abramowicz et al. 1995) as described in Boughelilba et al. (2022). ADAFs exist only when the accretion rate is sufficiently low ($\dot{m} = \dot{M}/\dot{M}_{\rm Edd} \leq 0.01$, where $\dot{m}$ is the mass accretion rate scaled to the Eddington accretion rate). The quantities governing the accretion flow depend on the plasma parameter β, which is the ratio between the gas and the total pressure (i.e., the sum of the magnetic and gas pressure), on the viscosity α and on the heating fraction δ_e which represents the fraction of viscous energy directly transmitted to the electrons of the plasma. Furthermore, we take $\dot{m} = \dot{m}_{\rm out}\,(R/R_{\rm out})^s$, where $R_{\rm out}$ is the outer radius of the ADAF and is associated with an accretion rate $\dot{m}_{\rm out}$, and s is the mass-loss parameter (Blandford & Begelman 1999).

4 Results

The ADAF spectrum is calculated for the two gamma-ray detected sources, as well as for the 23 other sources where X-ray data are available. The resulting SED is a combination of the ADAF component, the jet component and the host galaxy's modified blackbody. FR 0s' jets are expected to be less powerful than FR Is' and only mildly relativistic (Giovannini et al. 2023). Therefore the relative jet bulk velocity is set to $\beta_{\rm j} = 0.55$, and a jet inclination with respect to the line of sight of 20°. A summary of the ADAF and jet parameters is given in Table 1. In Figure 2, we present the SED of the two gamma-ray detected sources (LEDA 55267 and LEDA 58287) and their multiwavelength models for a jet magnetic field strength of 25 G from left to right respectively. As described above, the 23 subthreshold sources with X-ray data possess a modelled ADAF and a jet. All the 112 subthreshold sources are modelled with the same jet parameters. For each source, the observed flux is displayed in Figure 3 in faint purple. The average SED of the population is represented with the darker, wider purple curve. The steady-state jet power is estimated by $L'_{\rm jet,ss} = \pi R'^2_{\rm em} \Gamma^2_{\rm j} \beta_{\rm j} c \sum_i u'_i$ where $u'_{\rm i}$ is the energy density of

Table 1. Model parameters. $n'_{\rm inj,e(p)}$ is the electron (proton) number density injection rate. The minimum Lorentz factor of the primary electrons and protons is set to $\gamma' = 1$. $R_{\rm S}$ is the Schwarzschild's radius.

Parameters	$B = 25\,{\rm G}$	$B = 50\,{\rm G}$
α	0.1	0.1
β	0.99	0.99
s	0.1	0.1
$R_{\rm out}$	$5 \times 10^3\,R_{\rm S}$	$5 \times 10^3\,R_{\rm S}$
δ_e	5×10^{-3}	5×10^{-3}
$\dot{m}(R = R_{\rm out})$	$(6 - 20) \times 10^{-4}$	$(1 - 4) \times 10^{-3}$
$R'_{\rm em}$ (cm)	4.0×10^{15}	1.2×10^{15}
$E'_{\rm max,e}$ (MeV)	$(8.0 - 15) \times 10^3$	8.0×10^3
$E'_{\rm max,p}$ (GeV)	$(2 - 5.5) \times 10^9$	$(1.5 - 4) \times 10^9$
$p_{\rm e} = p_{\rm p}$	1.7	1.7
$u'_{\rm part,ss}/u'_{\rm B}$	$(3.5 - 21) \times 10^{-2}$	$(1 - 4.8) \times 10^{-1}$
$L'_{\rm jet,ss}$ (erg s^{-1})	$(3.1 - 3.6) \times 10^{43}$	$(1.1 - 1.5) \times 10^{43}$

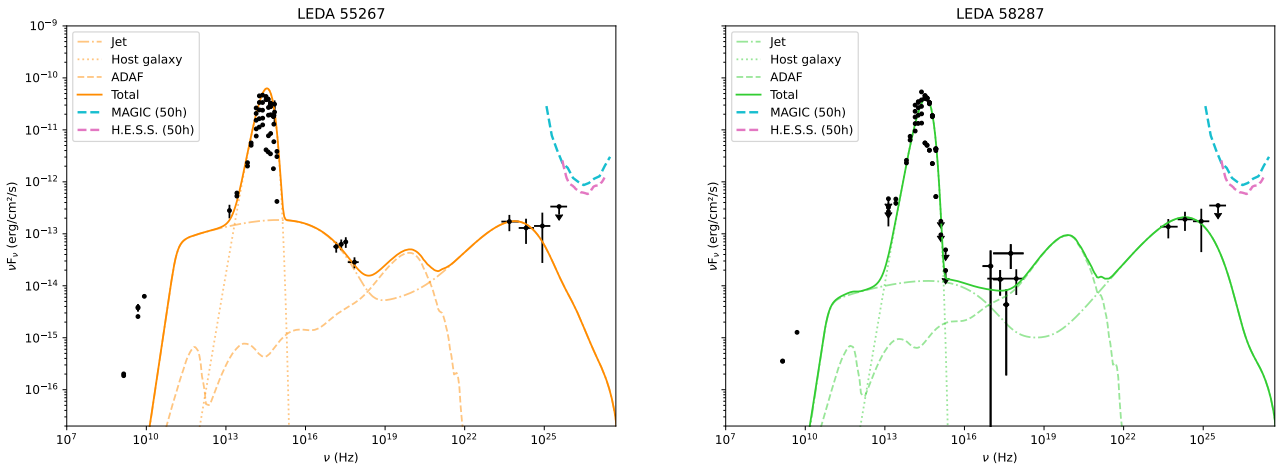

Fig. 2. Left: SED and models for a magnetic field strength of 25G in the jet for LEDA 55267. **Right:** For LEDA 58287. The dotted line is the modified blackbody modelling the host galaxy emission, the dashed line is the emission coming from the ADAF, the dash-dotted line is the total jet's emission and the solid line represents the total emission of the source and is the sum of the three components. The differential fluxes sensitivities for 50 hours of observation with MAGIC (Aleksić et al. 2016) and H.E.S.S (Holler et al. 2015) are shown with the cyan and pink dashed lines respectively.

radiation, electrons, protons ($u'_{\rm part,ss}$) and magnetic field ($u'_{\rm B}$) respectively. Overall, the jet composition is very close to equipartition.

5 Conclusion

We found that the broadband SED of FR 0s is extremely similar to the archetypal FR I, M87, during its quiet steady state (described in detail in EHT MWL Science Working Group et al. 2021). The similarity goes from the core radio emission to the X-ray band, and up to gamma-rays for two individual sources detected in the high-energy band. We found that a compact subparsec-scale jet-flow emission region is able to explain the nuclear multiwavelength SED of FR 0s, provided that a magnetic field strength of $25 - 50\,{\rm G}$ is reached in the core region. The jet of FR 0s is mildly relativistic, with a velocity $\beta_{\rm j} c = 0.55\,c$, which is consistent with the value obtained by Giovannini et al. (2023) when observing the core of FR 0s in comparison to FR Is.

This work acknowledges financial support from the Austrian Science Fund (FWF) under grant agreement number I 4144-N27. MB

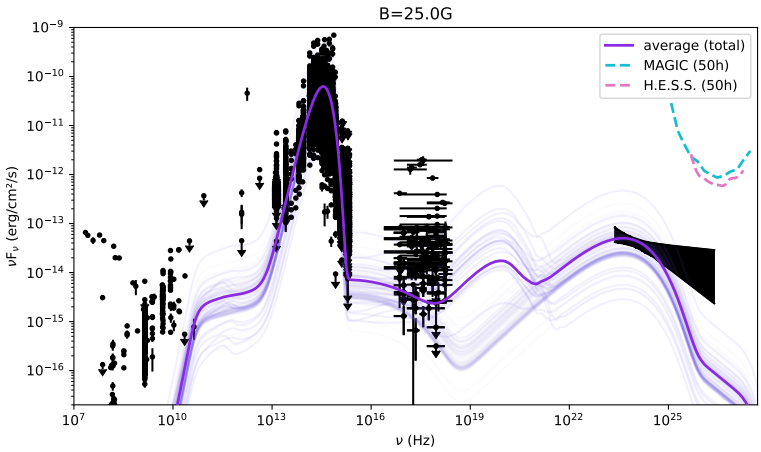

Fig. 3. SEDs of the 112 sources that are not individually detected in the gamma-ray band, and models for a magnetic field strength of 25G in the jet. The faint purple lines are the individual fluxes of the 112 sources (see main text for details) and the solid purple line is the average of the 112 models. The differential fluxes sensitivities for 50 hours of observation with MAGIC (Aleksić et al. 2016) and H.E.S.S (Holler et al. 2015) are shown with the cyan and pink dashed lines respectively.

has for this project received funding from the European Union's Horizon 2020 research and innovation program under the Marie Sklodowska-Curie grant agreement No 847476. The views and opinions expressed herein do not necessarily reflect those of the European Commission.

References

Abramowicz, M. A., Chen, X., Kato, S., Lasota, J.-P., & Regev, O. 1995, ApJ, 438, L37

Acciari, V. A., Beilicke, M., Blaylock, G., et al. 2008, ApJ, 679, 397

Aharonian, F., Akhperjanian, A. G., Bazer-Bachi, A. R., et al. 2006, Science, 314, 1424

Albert, J., Aliu, E., Anderhub, H., et al. 2008, ApJ, 685, L23

Aleksić, J., Ansoldi, S., Antonelli, L. A., et al. 2016, Astroparticle Physics, 72, 76

Aliu, E., Arlen, T., Aune, T., et al. 2012, ApJ, 746, 141

Baldi, R. D. & Capetti, A. 2009, A&A, 508, 603

Baldi, R. D. & Capetti, A. 2010, A&A, 519, A48

Baldi, R. D., Capetti, A., & Giovannini, G. 2019, MNRAS, 482, 2294

Baldi, R. D., Capetti, A., & Massaro, F. 2018, A&A, 609, A1

Blandford, R. D. & Begelman, M. C. 1999, MNRAS, 303, L1

Boughelilba, M., Reimer, A., & Merten, L. 2022, ApJ, 938, 79

Capetti, A., Massaro, F., & Baldi, R. D. 2017, A&A, 598, A49

EHT MWL Science Working Group, Algaba, J. C., Anczarski, J., et al. 2021, ApJ, 911, L11

Garofalo, D., Evans, D. A., & Sambruna, R. M. 2010, MNRAS, 406, 975

Garofalo, D. & Singh, C. B. 2019, ApJ, 871, 259

Giovannini, G., Baldi, R. D., Capetti, A., Giroletti, M., & Lico, R. 2023, A&A, 672, A104

Holler, M., de Naurois, M., Zaborov, D., Balzer, A., & Chalmé-Calvet, R. 2015, in International Cosmic Ray Conference, Vol. 34, 34th International Cosmic Ray Conference (ICRC2015), 980

Ichimaru, S. 1977, ApJ, 214, 840

MAGIC Collaboration, Acciari, V. A., Ansoldi, S., et al. 2020, MNRAS, 492, 5354

Merten, L., Boughelilba, M., Reimer, A., et al. 2021, Astroparticle Physics, 128, 102564

Narayan, R. & Yi, I. 1995, ApJ, 452, 710

Paliya, V. S. 2021, ApJ, 918, L39

Rees, M. J., Begelman, M. C., Blandford, R. D., & Phinney, E. S. 1982, Nature, 295, 17

Torresi, E., Grandi, P., Capetti, A., Baldi, R. D., & Giovannini, G. 2018, MNRAS, 476, 5535